Sixth International Symposium on Turbulence and Shear Flow Phenomena
Seoul, Korea, 22-24 June 2009

EXPERIMENTAL INVESTIGATION OF THE WAKE BEHIND A DISCONTINUOUS CYLINDER

V. S. R. Mandava[1], G. A. Kopp[2], J. Herrero[1], Francesc Giralt[1]

[1]Department d'Enginyeria Quimica
Universitat Rovira i Virgili
Av. Països Catalans 26, Tarragona, Catalunya, 43007, Spain
fgiralt@urv.cat

[2]Boundary Layer Wind Tunnel Laboratory
University of Western Ontario
London, Ontario, N6A 5B9, Canada
gakopp@uwo.ca

ABSTRACT

The effect of a discontinuous cylinder geometry on the near wake structures was investigated experimentally. This 'discontinuous' circular cylinder has gaps so that solid segments 5D long are followed by gaps 2.5D long, in a repeating pattern, where D is the diameter of the cylinder. A thin steel plate was used to hold all of the cylinder pieces together. Thus, a three-dimensional (3D) wake was created at the origin with the intent to force the near wake flow to have similar structural characteristics to the far wake behind an 'infinite' cylinder, i.e., a near wake flow with horseshoes or double rollers formed by rapid kinking of Kármán-like vortices. Since the kinetic energy associated with the fluctuations of these near-wake 3D vortical structures was high, the flow system was considered suitable to clarify the role of these velocity patterns in the entrainment process of wake flows, which is still the subject of controversy. Particle image velocimetry (PIV) measurements were made in the wake behind the discontinuous cylinder up to x/D=56, at a Reynolds number Re=10,000. The development of double rollers resulting from the interaction between the high momentum flow through the gaps and the Kármán-like vortices formed behind the solid cylindrical segments was confirmed. They have a dominant role in the initial wake growth which occurs under significant momentum transfer in the spanwise direction. This overall flow dynamics is similar to the momentum transfer that takes place at the scale of the intermittent turbulent bulges that protrude from the wake in the far region and that were reported to be associated with double rollers.

INTRODUCTION

Understanding the kinematics and dynamics of entrainment and mixing is important in many practical engineering situations. Entrainment has been considered by many researchers as a large-scale process (e.g., Townsend, 1976; Bevilaqua and Lykoudis, 1977) and several phenomenological descriptions have been proposed in the past. Examples are the vortex sheet roll-up due to a Kelvin-Helmholtz instability and entrapment of external fluid into the core of the vortex (Prandtl and Tietjens, 1934; Sreenivasan et al., 1989; Caulfield and Peltier, 2000); Townsend´s (1966, 1976) growth-decay model; 'sweeping' non-turbulent fluid into the turbulent region by rotational motions (Bevilaqua and Lykoudis, 1977). These theories or phenomenological models do not explain the role of large scale vortical structures in relation to the initial conditions that generate them. In contrast to the large-scale approaches to entrainment just mentioned, Mathew and Basu (2002) and Westerweel et al. (2005) concluded that the mechanism of entrainment process is dominated by small scales (nibbling). Thus, it is still not clear whether the entrainment process occurs as a result of outward spreading of small-scale vortices "nibbling" or by the action of large-scale eddies in the turbulent-non turbulent flow interfacial region.

Wakes are an ideal flow system to study the genesis of large scale vortices and their dynamical evolution with respect to initial flow conditions. The instability and transition in the near wake has been studied by many researchers (e.g., Gerrard, 1967; Roshko and Fiszdon, 1969; Mc Crosky, 1977; Zdravkovich, 1990; Williamson, 1996; Norberg, 2003; Dong, 2006). Several numerical and experimental studies have also been carried out in the past to characterize the three-dimensional (3D) nature of wake flows and vortex shedding by exciting 3D modes at the originating body (e.g., Bearman and Tombazis, 1993; Bernman and Owen, 1998; Darekar and Sherwin, 2001; Lam et al., 2004; Wu et al., 2005; Lee and Nguyen, 2007; Ling and Lin, 2008). Control of initially perturbed wake flows has also raised attention (e.g., Dobre et al., 2006). A more radical initial perturbation in a 2D wake flow behind an infinite body in the spanwise direction could be attained by alternating solid with discontinuous segments of the same body in a repeating pattern. This would have the benefit of not changing the basic body geometry that generates the wake flow.

In the current study we have considered a 3D cylinder configuration with gaps, i.e., pieces of equidistant cylinders

along the cylinder center axis. With this arrangement part of the free stream flow passes through the gaps while the rest passes over the 3D cylinder pieces forming a 3D wake. The free stream flow through the gaps would move inwards towards each wake behind the cylindrical pieces due to pressure gradients. Simultaneously, Kármán-like vortices would be formed behind the solid segments together with other vortical structures at both ends. This new configuration of the initial flow conditions should cause the lifting or kinking of the segmented, 3D Kármán-like vortices and horseshoe/double-rollers/o-ring kind of vortices would be generated in the near wake. These are the vortices that usually occur in the far wake region behind an infinite cylinder (e.g., Ferré and Giralt, 1988; Giralt and Ferré, 1993; Vernet et al., 1999; Kopp et al., 2002). As a consequence, the current flow configuration may help explaining how double rollers could be generated earlier in the wake, how they evolve with respect to initial flow conditions, and shed light on the entrainment and mixing mechanisms in turbulent free flows.

EXPERIMENTAL DETAILS

A portion of the experiments were carried out at the Boundary Layer Wind Tunnel Laboratory (BLWTL), University of Western Ontario, Canada, while the remaining experiments were conducted in the open return wind tunnel of the Chemical Engineering Department at the Universitat Rovira i Virgili in Tarragona. At both places, measurements were conducted with the same discontinuous cylinder model and at the same free-stream velocity U = 9.2m/s, thus, at the same Reynolds number Re = 10^4. The diameter (D) of the cylinder pieces was 0.0163m, the length of each segment was 5D, and the gap between the cylinder pieces was 2.5D. A thin steel plate, whose thickness was 0.81mm and width equal to the cylinder diameter, held the cylinder pieces together without interfering significantly with the dominant 3D flow structure upstream and downstream of the model. The dimensions of the model and co-ordinate system used are shown in Fig. 1. At Re = 10^4 the boundary layer is laminar and the near wake is fully turbulent (Dimotakis, 2000). Particle image velocimetry (PIV) was used to measure the instantaneous velocity field in the wake region with a flash lamp laser of frequency 15Hz to illuminate particles in the flow.

First, several measurements were conducted in Canada, in the near wake region up to 8.5 diameters downstream on transverse(x-y) planes, along the cylinder axis. Planes at every half a diameter width, from center of the middle cylinder piece (z/D=0) to the end of the middle cylinder piece (z/D=2.5), were examined. Two measurements were carried out within the gap region between cylinder pieces, one at 0.5D away from the edge of the cylinder piece (i.e., at z/D=3.0) and the other at the center of the gap region (z/D=3.75). Several experiments were carried out on transverse(x-y) planes to check flow symmetry.

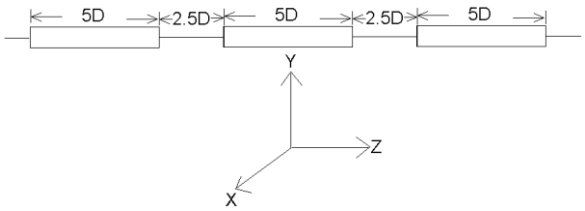

Figure 1. Cylinder model and co-ordinate system

The experiments were repeated with stereo particle image velocimetry in Tarragona, Spain, with the same discontinuous cylinder configuration (Fig. 1) but with five cylinder pieces, instead of the three in the earlier setup. The data obtained were in reasonable agreement with the earlier experimental data determined in Canada.

Measurements were extended in Tarragona to further downstream in the wake on several vertical (x-y) planes, x/D=9 to 16, 26 to 36 and 43 to 56, at the middle plane of the discontinuous cylinder (z/D=0). Experiments were also conducted on the horizontal (x-z) planes in the downstream wake from x/D=10 to 20 at y/D=2, and 27 to 36 at y/D=3. Data for the corresponding wake of an infinite cylinder were also collected at all the vertical and horizontal planes. The aspect ratio of the infinite cylinder was 37 and the blockage in the tunnel was 2.7%. The TSI Insight3G software was used, in all cases, for frame to frame correlation to generate instantaneous velocity fields, with an interrogation window of size 32 x 32 pixels with 50% overlap. These instantaneous velocity fields were then ensemble averaged to determine the mean streamwise and transverse velocities, root mean square (r. m. s) velocity fluctuations, mean Reynolds shear stresses and mean z-vorticity patterns on all the transverse (x-y) and horizontal (x-z) planes. The instantaneous data on horizontal planes were used to identify the footprints of double rollers in the near wake.

RESULTS

Current data for the infinite cylinder were compared and found in reasonable agreement with the literature measurement (Dong et al., 2006; Norberg, 1998). In the following sections discontinuous and infinite cylinder data are compared. The plots presented in the paper are, unless specified, on transverse planes at z/D=0. In all contour plots flow direction is from left to right and, positive and negative magnitude of contours are indicated by solid and dashed lines, respectively.

For the discontinuous cylinder case, note that the velocity defect and vorticity levels at the wake behind the steel plate are much smaller than those at the wake behind each cylinder piece (Fig. 2), and their effects on wake data were neglected.

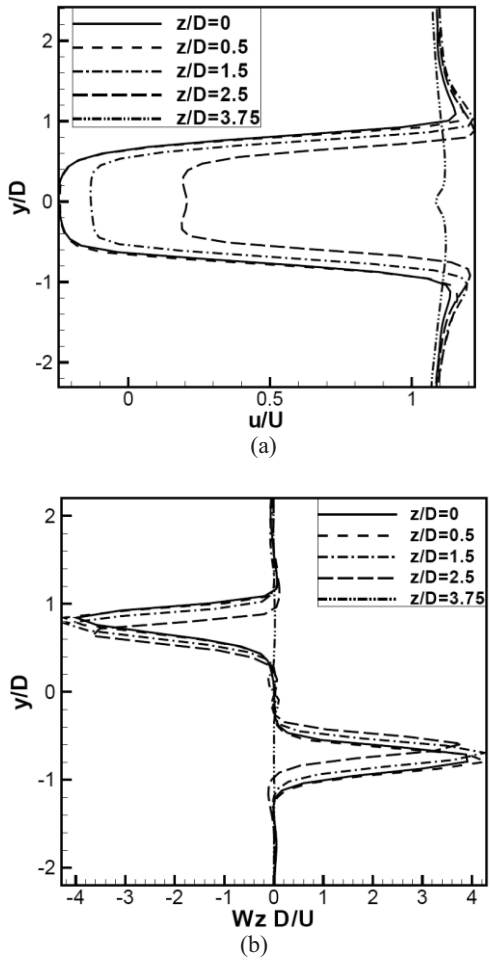

Figure 2. (a) Profiles of mean streamwise velocity (u/U) at x/D=1; (b) Profiles of mean z-vorticity (w_zD/U) at x/D=1

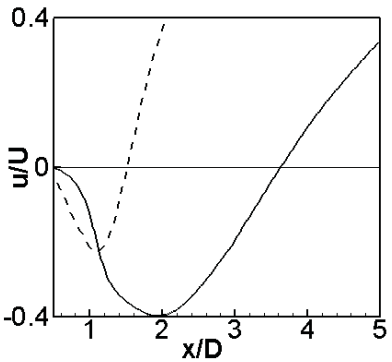

Figure 3. Mean stramwise velocity (u/U) at wake center line (y/D=0) of discontinuous (—) and infinite (----) cylinders

Wake characteristics

The variations in base suction are associated with variations in vortex formation length. It is the distance between separation point and the location at which the vortex is fully formed, before it is shed (Gerrard 1966). Definitions of the formation length are given elsewhere (Bloor, 1966; Woo et al., 1983; Norberg, 1986 and 1998; Govardhan, 2001). The formation length of the wake for the discontinuous cylinder is 3.62D, and the corresponding value for the infinite cylinder is 1.5D by the present experiments and 1.52D by Norberg (1998). As in the reference Norberg (1998), we have used time averaged closure point (point of zero u/U at wake centerline in Figure 3) to measure the formation length.

The mean streamwise velocities at wake center line (Fig. 3) show strong negative values (reverse flow) in the wake region. The magnitude of the minimum velocity and the location where this occurs are different from the infinite cylinder case. The maximum magnitude of the negative velocity is 0.4 and the corresponding value for the infinite cylinder is 0.225 in the current experiments, 0.228 in Dong et al. (2006) from their 2D PIV experiment, and 0.38 in Norberg (1998) from Laser Doppler Velocimetry (LDV) analysis. The width of the wake at x/D=1.5 is much wider than the wake behind an infinite cylinder (Fig. 4a). The wake has more velocity deficit in the region close to the cylinder when compare to the infinite cylinder case, but as the wake grows downstream it recovers quickly (Fig. 4).

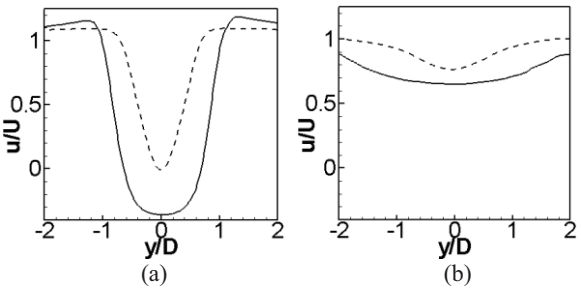

Figure 4. Comparison of mean streamwise velocity in discontinuous (—) and infinite (----) cylinder at (a) x/D=1.5; (b) x/D=8

The u′ and v′ are the streamwise and transverse root mean square velocities. The magnitude of the maximum fluctuations of the normalized root mean square streamwise velocity (u′/U) for the discontinuous cylinder is smaller. The corresponding location is displaced further downstream compared to the infinite cylinder case. The maximum value is 0.30 and occurs at x/D=2.5. The corresponding values for the infinite cylinder are 0.45 at x/D=1.4 in the current experiments, 0.5 at x/D=1.14 in Dong et al. (2006) and 0.43 at x/D=1.5 in Norberg (1998).

The double peak behavior in the streamwise normal stress in Fig 5 arises as a result of the alternating nature of the shed vortices and the formation of a 3D vortex street with kinked Kármán-like vortices. As the wake flow develops, the peaks become less and less prominent. The wake characteristics remain similar along the cylinder axis at x/D=1 (Fig. 2), but at further downstream positions, for example at x/D=5, it is clear from Fig. 5 that the peaks of stream-wise normal stress slowly disappear; the peaks at the plane z/D=1.5 are less prominent than at the middle plane z/D=0 because of the momentum input occurring through the gaps into the wake.

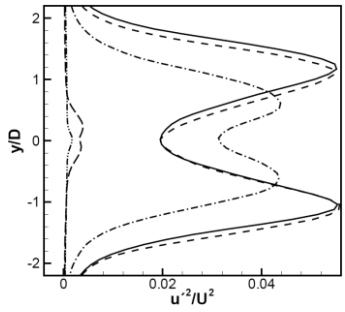

Figure 5. The profiles of mean streamwise Reynolds normal stress at x/D=5, z/D=0 (—), z/D=0.5 (----), z/D=1.5 (-.-.-.-), z/D=2.5 (– – –) and z/D=3.75 (-..-..-..-)

The dominant peak level of normalized Reynolds shear stress ($u'v'/U^2$) is smaller and the corresponding location displaced downstream in wake of the discontinuous cylinder wake compared to the infinite cylinder flow situation. The peak level is 0.05 and it occurs at location x/D=3, while the corresponding values for the infinite cylinder are 0.12 at x/D=1.64 in the present experiments and 0.14 at x/D=1.4 in Dong et al. (2006). The contour patterns of the normalized shear stress ($u'v'/U^2$) for the discontinuous cylinder, not shown here, show that regions of high shear have moved relatively away from the cylinder surface compared to the infinite cylinder case. This may be related to the converging streamlines in the wake from ends of the cylinder segments. Velocity fluctuations are largest at the vortex centers. When Vortices are shed into the near wake and are advected downstream they move away from the centerline.

Entrainment process

The flow around a short cylinder segment is essentially three-dimensional. The end effects play a dominant role and strongly modify the structure of vortices in the near wake region. Initially the evolving Kármán-like vortices are connected to the ends of the cylinder. When shed from the cylinder they are kinked and form a horseshoe like structure that may reconnect, due to converging streamlines in the wake, and form a vortex-ring-like structure. At times, these vortices can be strongly distorted, which may result in a much more complicated flow pattern.

The horseshoe eddy is a structure with two legs which are shear aligned and connected at the top with spanwise vorticity. The cross-section of the two legs forms a double roller pattern on the horizontal plane. These double roller structures, which are known to appear in the far wake region behind an infinite cylinder, are also observed in the near wake (xD≈15) of the discontinuous cylinder, as shown in Fig.6. The vectors of streamwise and spanwise velocity fluctuations on horizontal (x-z) plane clearly depict in this figure the footprints of double roller vortices early in the discontinuous wake development. Similar kind of double roller structures are found on the horizontal plane further downstream (xD≈30) behind the discontinuous cylinder, as shown in Fig. 7. This indicates that once formed they remain because are capable of extracting energy by stretching while diffusing in the spanwise direction and moving downstream by advection.

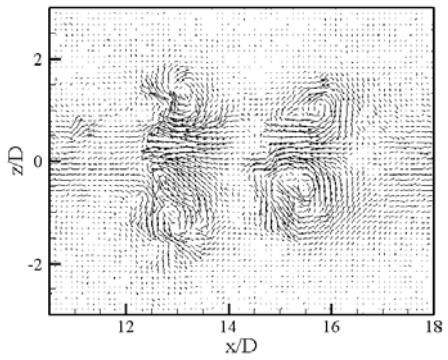

Figure 6. The normalized (u,w) velocity fluctuations in the near wake behind the discontinuous cylinder

The corresponding spanwise profiles of y-vorticity and u'w' shear stress are presented in Fig. 8. The flow of high momentum fluid entering the wake through the gaps, which moves towards the regions behind the cylinder segments, causes a lift upwards and downwards of the alternating Kármán-like vortices that these segments shed. As a result, the initially dominant z-vorticity projects into y-vorticity at the central z-x plane. Fig. 8a shows how this y-vorticity decreases with x/D as double rollers are advected downstream and diffuse. The u'w' shear stress also diminishes with x/D (Fig. 8b). which is indicative of the wake evolution towards fully development ($u'w'/U^2=0$).

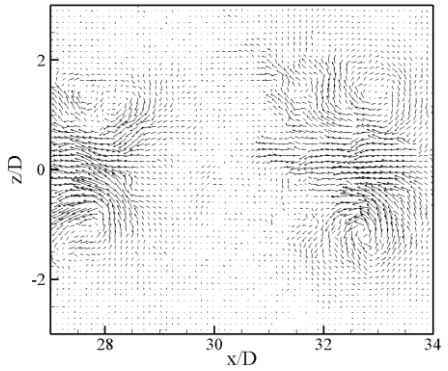

Figure 7. The normalized (u,w) velocity fluctuations in the medium far wake behind the discontinuous cylinder.

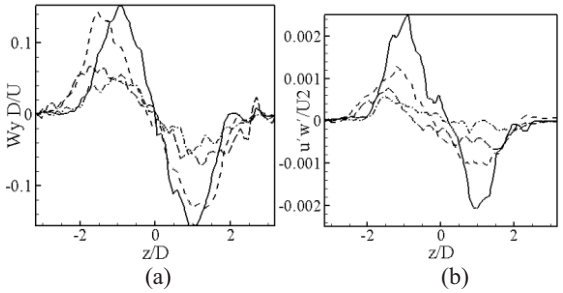

Figure 8. The profiles of (a) mean y-vorticity (Wy D/U), at x/D=11 (—), x/D=19 (----), x/D=28 (-.-.-.-) and x/d=36 (– – –); (b) mean shear stress ($u'w'/U^2$), at x/D)=11 (—), x/D=19 (----), x/D=28 (-.-.-.-), and x/D=36 (– – –)

Double rollers are responsible for maintaining the correlation between the streamwise and lateral velocity fluctuations, with correlation being largest at the center plane of the structure (Vernet et al., 1997). The profiles of normalized shear stress ($u'v'/U^2$) at several downstream locations on wake center line are shown in Fig. 9. The shear stress peaks close to the wake formation length at x/D=3, and then decreases as x/D increases. Again, the input of momentum by the high velocity flow in the gap seems evident.

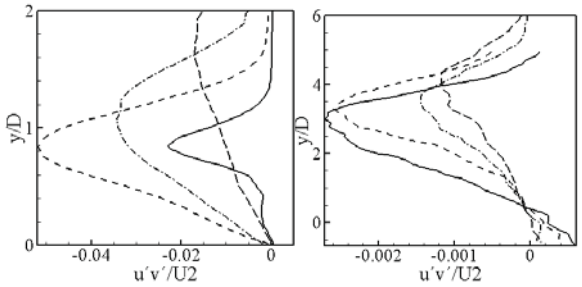

Figure 9. The profiles of mean shear stress ($u'v'/U^2$) at (a) x/D=1.5 (—), x/D=3 (----), x/D=5 (-.-.-.-) and x/d=8 (– – –); (b) x/D)=26 (—), x/D=32 (----), x/D=44 (-.-.-.-), and x/D=56 (– – –)

The profiles of mean spanwise vorticity (Wz D/U) at several downstream stations are shown in Fig. 10. The magnitude of negative vorticity is maximum close to the cylinder, and decreases in magnitude as the wake gradually develops. Profiles in the downstream wake reflect, with maximum negative vorticity values, the mean path of the top of the horseshoe vortices which have high spanwise negative vorticity.

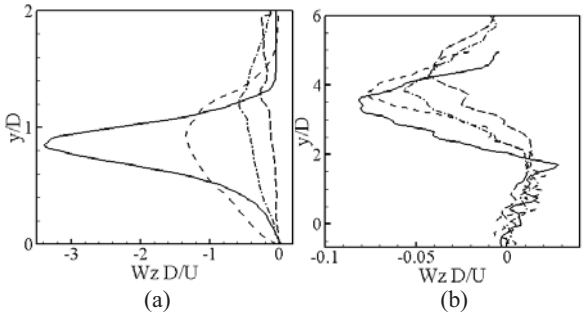

Figure 10. The profiles of mean z-vorticity (W_z D/U) at (a) x/D=1.5 (—), x/D=3 (----), x/D=5 (-.-.-.-) and x/d=8 (– – –); (b) x/D)=26 (—), x/D=32 (----), x/D=44 (-.-.-.-), and x/D=56 (….)

Finally, Fig. 11 shows that the wake thickness and growth rate in the current discontinuous cylinder case are both larger than for the 2D cylinder wake. These results illustrate the important role of large scale 3D motions, such as double rollers, in the entrainment process. LES calculations not reported here are in agreement with experimental data.

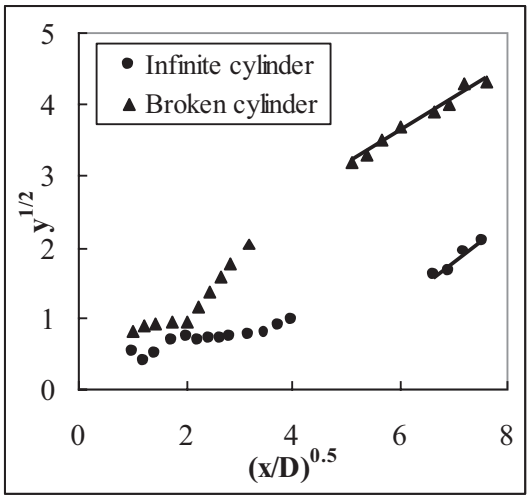

Figure 11. Variation of the wake half-width with streamwise location for both the discontinuous and 2D cylinder

CONCLUSIONS

The effect of inflow conditions on the near wake structure behind a discontinuous cylinder, at Reynolds number 10,000 was investigated experimentally. The flow statistics such as mean velocities, r. m. s. velocity fluctuations, mean Reynolds shear stress and mean z-vorticity of the discontinuous cylinder have been compared with the corresponding data for an infinite cylinder wake. The wake bubble behind the segments of the discontinuous cylinder, which is indicative of reverse flow, is significantly longer than that for the infinite cylinder, i.e; the formation length is enlarged. This delay shedding may be related to the converging streamlines in the wake from ends of the cylinder due to the inflow of high momentum fluid through the gaps. The wake width of the discontinuous cylinder is much wider and grows faster than that for the infinite cylinder. The velocity deficit is larger in the near wake region, but as the wake grows downstream it recovers quickly. The peaks of the streamwise normal stress are less prominent as wake grows downstream. Once Kármán-like vortices are shed they are kinked in the very-near wake due to effect of the flow input through the gaps and form double rollers. Footprints of double-roller vortices have been unambiguously identified on the horizontal planes in the wake of the discontinuous cylinder, both from experimental data and LES results not reported here.

ACKNOWLEDGMENT

The current study was supported by the grants FIS2005-07194 and CTQ2008-04857/PPQ (MEC, Spain) and 2005SGR-00735 (DURSI, Generalitat de Catalunya). Francesc Giralt acknowledges the Distinguished Researcher Award, Generalitat de Catalunya. Gregory Kopp gratefully acknowledges the support of the Canada Research Chairs Program.

REFERENCES

Bearman P.W., Tombazis N., 1993, The effects of 3-dimensional imposed disturbances on bluff-body near wake flows, *Jounal Wind Engineering and Industrial Aerodynamics*, Vol. 49(1-3), pp. 339-349.

Bearman P.W., Owen J.C., 1998, Reduction of bluff-body drag abd suppression of vortex shedding by the introduction of wavy separation lines, Jounal of Fluids and Structures, Vol. 12, pp. 123-130.

Bevilaqua P.M., Lykoudis P.S., 1977, Some observation on the mechanisms of entrainment, AIAA Journal, Vol. 15, pp. 1194-1196.

Bloor S., 1966, The transition to turbulence in the wake of a circular cylinder, Journal of Fluid Mechanics, Vol. 19, pp. 290-304.

Caulfield C.P., Peltier W.R., 2000, The anatomy of mixing transition in homogeneous and stratified free shear layers, Journal of Fluid Mechanics, Vol. 413, pp. 1-47.

Darekar R.M., Sherwin S.J., 2001, Flow past a bluff body with a wavy stagnation face, Journal of Fluids and Structures, Vol. 15(3-4), pp. 587-596.

Dimotakis P.E., 2000, The mixing transition in turbulent flows, Journal of Fluid Mechanics, Vol. 409, pp. 69-98.

Dobre A., Hangan H., Vickery B.J. 2006 Wake control based on spanwise sinusoidal perturbations, AIAA Journal, Vol. 44(3), pp. 485-492.

Dong S., Karniadakis G.E., Ekmekci A., Rockwell D., 2006, A combined direct numerical simulation – particle image velocimetry study of the turbulent near wake, Journal of Fluid Mechanics, Vol. 569, pp. 185-207.

Ferré J.A., Giralt F., 1988, Pattern recognition analysis of the velocity field in plane turbulent wakes, Journal of Fluid Mechanics, Vol. 198, pp. 27-64.

Gerrard J.H., 1966, The mechanics of the vortex formation region of vortices behind bluff bodies, Journal of Fluid Mechanics, Vol. 25, pp. 401-413.

Gerrard J.H., 1967, Experimental investigation of separated boundary layer undergoing transition to turbulence, Physics of Fluids, Vol. 10, pp. S98-100.

Giralt F., Ferré J.A., 1993, Structure and flow pattern in turbulent flow, Physics of Fluids, Vol. A5, pp. 1783-1789.

Govardhan R., Williamson C.H.K., 2001, Mean and fluctuating velocity fields in the wake of a freely vibrating cylinder, Journal of Fluids and Structures, Vol. 15, pp. 489-501.

Kopp G.A., Giralt F., Keffer J.F, 2002, Entrainment vortices and interfacial intermittent turbulent bulges in a plane turbulent wake, Journal of Fluid Mechanics, vol. 469, pp. 49-70.

Lam K., Wang F.H., Li J.Y., So R.M.C., 2004, Experimental investigation of the mean and fluctuating forces of wavy (varicose) cylinders in a cross-flow, Journal of Fluid and Structures, Vol. 19(3), pp. 321-334.

Lee S.J., Nguyen A.T., 2007, Experimental investigation on wake behind a wavy cylinder having sinusoidal cross-sectional area variation, Fuid Dynamics Research, Vol. 39(4), pp. 292-304.

Ling G.C., Lin L.M., 2008, A note on the numerical simulations of flow past a wavy square-section cylinder, Acta Mechanica Sinica, Vol. 24(1), pp. 101-105.

Mathew J., Basu A.J., 2002, Some characteristics of entrainment at a cylindrical turbulence boundary, Physics of Fluids, Vol. 14, pp. 2065-2072.

McCroskey W.J., 1977, Some current research in unsteady fluid dynamics – the 1976 freeman scholar lecture, Journal of Fluids Engineering, Vol. 99, pp. 8-39.

Norberg C., 1986, Interaction between freestream turbulence and vortex shedding for a single tube in cross flow, Journal of Wind engineering And Industrial Aerodynamics, Vol. 23, pp. 501-514.

Norberb C., 1998, LDV-measurements in the near wake of a circular cylinder, Advances in understanding of bluff body wakes and vortex induced vibrations, Washington DC, June 1998.

Norberg C., 2003, Fluctuating lift on a circular cylinder: review and new measurements, Journal of Fluids and Structures, Vol. 17, pp. 57-96.

Prandtl L., Tietjens O.G., 1934, Fundamentals of hydro- and aeromechanics, United engineers Trustees.

Roshko A., Fiszdon W., 1969, On the persistence of transition in the near wake, Problems of Hydrodynamics and Continuum Mechanics, pp. 606-616. SIAM

Sreenivasan K.R., Ramshankar R., Meneveau C., 1989, Mixing, entrainment and fractal dimensions of surfaces in turbulent flows, Proc. R. Soc. Lond. A, Vol. 421, pp. 79-108.

Townsend A.A., 1976, The structure of turbulence shear flow, 2nd edn. Cambridge University Press.

Townsend A.A., 1966, The mechanism of entrainment in free turbulent flows, Journal of Fluid Mechanics, Vol. 26, pp. 689-715.

Vernet A., Kopp G.A., Ferré J.A., Giralt F., 1999, Three-dimensional structure and momentum transfer in a turbulent cylinder wake, Journal of Fluid Mechanics, Vol. 394, pp. 303-337.

Vernet A., Kopp G.A., Ferré J.A., Giralt F., 1997, Simultaneous velocity and temperature patterns in the far region of a turbulent cylinder wake, Journal of fluids Engineering, Vol .119, pp. 463-466.

Westerweel J., Fukushima C., Pedersen J.M., Hunt, J.C.R., 2005, Mechanics of the turbulent and non-turbulent interface of a jet, Physical Review Letters, Vol. 17, pp. 174501.

Williamson C.H.K., 1996, Vortex dynamics in a cylinder wake, Annual Review of Fluid Mechanics, vol.28, pp. 477-539.

Wu S.J., Miau J.J., Hu C.C., Chou J. H, 2005, On low-frequency modulations and three-dimensionality in vortex shedding behind a normal plate, Journal of Fluid Mechanics, Vol. 526, pp. 117-146.

Woo H.G., Cermak J.E., Peterka J.A., 1993, On vortex locking-on phenomenon for a cable in linear shear flow , Journal of Wind Engineering and Industrial Aerodynamics, Vol. 14, pp. 289-300.

Zdravkovich M.M., 1990, Conceptual over view of laminar and turbulent flows past smooth and rough cylinders, Journal of Wind Engineering and Industrial Aerodynamics, Vol. 33, pp. 53-62.